Beamforming of supersonic jet noise for crackle-related events

Aaron B. Vaughn, Kent L. Gee, S. Hales Swift, Alan T. Wall, J. Micah Downing, and Michael M. James

---

ARTICLES YOU MAY BE INTERESTED IN

Noise: Paper 1aNS4

(Special Session: Supersonic Jet Aeroacoustics I)

Beamforming of supersonic jet noise for crackle-related events

Aaron B. Vaughn, **Kent L. Gee and S. Hales Swift**
Department of Physics and Astronomy, Brigham Young University, Provo, UT, 84602;
aaron.burton.vaughn@gmail.com; kentgee@byu.edu; hales.swift@gmail.com

Alan T. Wall
Battlespace Acoustics Branch, Air Force Research Laboratory, Wright-Patterson Air Force Base, OH,
45433; alan.wall.4@usaf.mil

J. Micah Downing and Michael M. James
Blue Ridge Research and Consulting, LCC, Asheville, NC, 28801; micah.downing@blueridgeresearch.com;
michael.james@blueridgeresearch.com

Crackle is an annoying perceptual component of supersonic jet noise. In the far field, crackle is related to the presence of acoustic shocks that develop due to nonlinear propagation, however, the intermittent source events that drive crackle generation are not well understood. This study investigates the apparent source locations of events related to crackle, which include high-amplitude or steepened, shock-like waveforms. The measured data were obtained through ground-array measurements near a high-performance military aircraft. The apparent source regions corresponding radiation angle, the skewness of the time-derivative of the pressure waveform (dSk), and overall sound pressure level are defined. Waveforms consisting of a dSk greater than 3 are considered to contain crackle. For 75% engine thrust request, the apparent source region for the top 1000 derivative events beamformed from locations with high derivative skewness, which corresponds to the potential for crackle, is 2-7 m downstream of the nozzle along the jet axis.

1. INTRODUCTION

This paper examines the spatial origin of events that relate to the development of crackle. Crackle is an annoying[1] and dominant[2] component of supersonic jet noise. Ffowcs Williams *et al.*[1] described crackle perceptually as "a rasping fricative sound," "the sound of … a badly connected loud speaker," and as "a startling staccato of cracks and bangs." Previous investigations have used experimental and computational means to better understand components of the crackle phenomenon such as its physical[3-9] and perceptual origins[10-12] and characteristics.[13-17] These studies have reached different conclusions regarding crackle due, in part, to their varying definition of the crackle phenomenon.[17] Thus, for this paper, we define crackle at the outset as a perceptual quality of the broadband noise that is related to the reception of acoustic shocks.[18,19] This is consistent with Ffowcs Williams *et al.*'s assertion that the "physical feature of a sound wave that gives rise to the readily identifiable subjective impression of 'crackle' is shown to be the sharp shocklike compressive waves that sometimes occur in the wave form."[1]

Acoustic shocks are characterized by large positive pressure derivatives and may result at the source, near the source, or in the far field through nonlinear propagation. Although the large derivatives are the cause of the crackle precept,[18] high-amplitude sound pressures give rise to shock formation and the presence of crackle in the far field.[20-24] This perception of crackle by far-field observers is of primary importance here because of its connection to community annoyance. Despite the motivation of observing crackle in the far field, it is helpful to look at near-plume characteristics that contain or are likely to produce shocks and are therefore drivers of far-field crackle. Some have looked at shocks near and in the jet plume,[4-6,24] while others have observed the formation of pressure skewness[3] in attempts to examine the physical and spatial source of crackle. It is presently unclear which transient events in the plume are responsible for far-field crackle, therefore both shocks present in the near field and high-pressure events that may develop shocks in the far field will be considered.

To look at these events, this study examines large derivative and large pressure events that are likely to be related to far-field characteristics of perceived crackle using "event-based" beamforming. This event-based beamforming combines conditional sampling of the waveform using high-amplitude pressures and derivatives as triggers to obtain short waveform segments containing the events, and time-domain beamforming via cross correlation of the waveform segments between pairs of adjacent microphones. A brief summary of the acoustical measurement of the F-35B high-performance military aircraft is provided, followed by a description of the methodology used in the beamforming process. Results for a single engine condition are then discussed, with concluding remarks at the end.

2. MEASUREMENT

Acoustical data were collected from an F-35B at Edwards Air Force Base in September 2013. James *et al.*[25] described the extensive measurement setup in Ref. [25], which had microphones located as close as 6.1 m to the jet shear layer and as far away as 1220 m. Sound measurements of a stationary aircraft were taken for multiple run-ups at each engine condition, which ranged from idle to maximum afterburner, or 150% engine thrust request (ETR). Across the 5-6 runups for each engine condition, there was less than ± 1 dB level variance.

This paper focuses on data acquired for a single engine condition at a 71-element, linear ground array located approximately 8-10 m from the estimated shear layer of the F-35B, shown in Fig. 1. The array consisted of GRAS 6.35 mm (1/4") Type 1 microphones which spanned 32 m with a

0.45 m inter-microphone spacing. Jet inlet angles were defined for each microphone location relative to the microphone array reference point (MARP), which was set to approximately 7.5 nozzle diameters downstream of the nozzle exit plane to be consistent with prior measurements.[21] This definition of a MARP better represents the primary noise source than the nozzle itself and is therefore used to define angles. Calibrated acoustic pressure waveform data were synchronously acquired for 27 s with National Instruments PXI-4498 cards sampling at 204.8 kHz. This paper focuses on data from 75% ETR; other engine conditions will be analyzed as part of a future paper submitted to the 2019 AIAA Aeroacoustics Meeting.
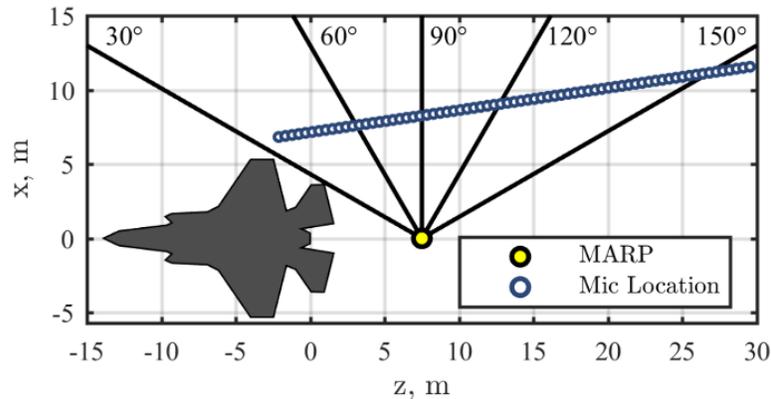

Figure 1. Measurement schematic of the 71-element linear ground array, approximately 8-10 m from the estimated jet shear layer. Inlet angles are defined relative to the microphone array reference point (MARP).

3. METHODS

The event-based beamforming method used in this paper consists of adjacent two-microphone cross correlation of a defined event to beamform selected events from the microphone array to the jet axis. This approach is related to the method used by Schlinker *et al.*[7,8] to observe, from the maximum radiation direction, the apparent acoustic source strength along the jet axis of laboratory and full-scale jets. For the method in this paper, events of interest are first defined, and then a window is applied around each event. A cross correlation is then performed with the resulting angle traced back to the jet centerline to find the apparent origin.

Three event types of interest are defined as follows: evenly-spaced, maximum pressure, and maximum derivative events. Events that are evenly spaced in time, and not tied to any specific pressure or derivative characteristics, should show where the general noise energy appears to be originating from and provide a baseline comparison for the other event types. High pressure events are more likely to steepen into far-field shocks via nonlinear propagation, whereas high derivatives correspond to the most shock-like events already developed within the recorded waveform. A set number of events are found in each upstream microphone and compared with the microphone immediately downstream to it after applying a time-lag and a window. Increasing the number of events decreases the significances of the events, and after an initial study to determine an appropriate number of events (ranging from 20 – 2000), the number of events chosen for this analysis was 1000 within each 27-s waveform. The spacing around events is also restricted to prevent their occurrence within 2.4-ms of another event of the same type. In this way the same event does not become overly emphasize, though events may occur simultaneously or independent of other event types. This is can be seen in a 40-ms waveform of defined events in Fig. 2. Top pressure and derivative events both deal with positive values, as the waveform is positively skewed for both the pressure time series and its derivative. Therefore, the top pressure events are found at the positive extremes, large derivatives occur in the middle of the high positive acoustic shocks,

and the evenly-spaced scenes are generally centered about lower pressure values than the other event types.
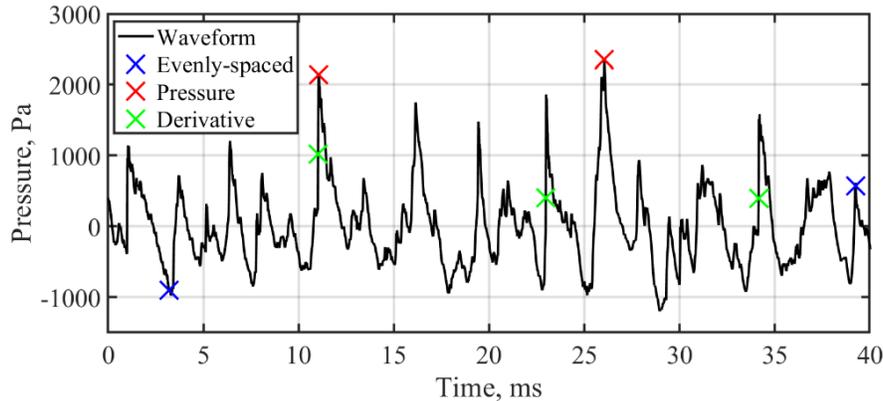
Figure 2. A 40-ms waveform clip with marked locations of the three defined event types.

After events are defined, a Hann window is applied to the waveform surrounding each event. The choice of a Hann window emphasizes the event that is centered within the reference waveform segment, and with the window being 20-ms long, the window should be large enough that in the case the event in the nonreference channel were shifted slightly from expected, it should be able to capture the relevant event. This also means that due to the window length, high pressure values may exist within windowed high derivative events and vice versa. An example of a windowed waveform is shown in Fig. 3.
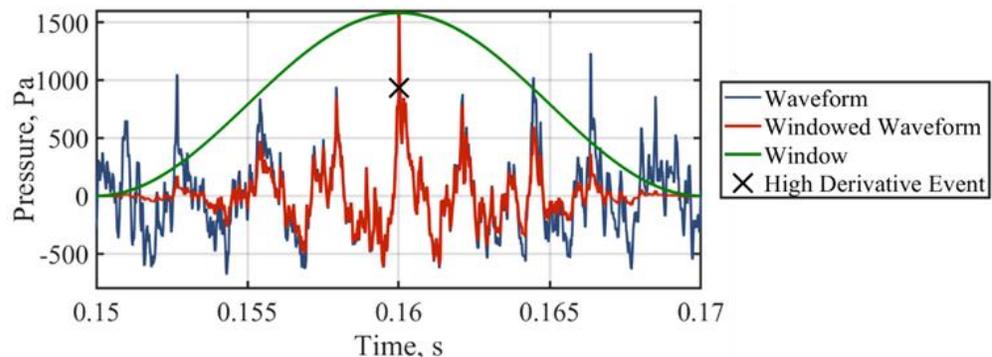
Figure 3. A 20-ms waveform clip illustrating the application of a window around a high derivative event at "X". Blue line indicates the unaltered waveform, the red line shows the windowed waveform, and the green line represents the window shape.

To obtain the apparent origin for each windowed waveform, a two-microphone cross correlation method is used as a time-domain beamformer. From the cross correlation, a time delay, $\Delta\tau$, due to the difference in arrival time between the two adjacent microphones is found. Then, using the assumption that waves in the vicinity of the microphones are locally planar and travelling at the speed of sound, c, a distance, $c\Delta\tau$, is found to form a right angle between the arrival path to the downstream microphone and the upstream microphone (as seen in Fig. 4). From the offset angle, ϕ, and the angle of incidence, ψ, the jet inlet angle, θ, is then found. Tracing the incident angle back to the jet centerline gives an apparent origin of the event. Each location and angle occurrence found via the event-based beamforming for each of the adjacent microphone pairs are then recorded and compiled into normalized histograms.
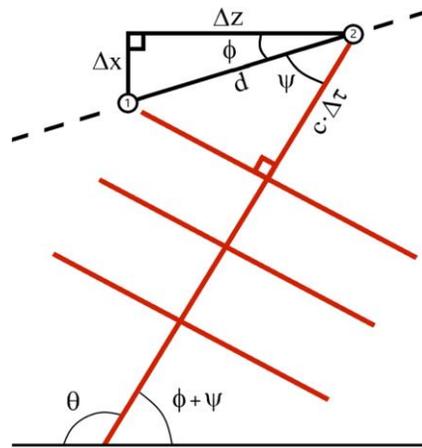
Figure 4. Schematic depicting the adjacent two-microphone cross correlation beamforming method.

4. RESULTS

Examples of waveforms containing acoustic shocks and those without shocks, similar to those depicted by Ffowcs Williams *et al.*[1], but from the F-35B at 75% ETR, are shown in Fig. 5. Each clip comes from a different location, is 50-ms in length, and is normalized by the maximum pressure within each waveform. The shock-containing waveform example comes from a microphone in the maximum radiation direction and is shown in Fig. 5a, whereas the non-shock-containing waveform in Fig. 5b comes from the farthest upstream microphone location. Shocks in Fig. 5a are characterized by a sudden increase from slightly negative to high positive amplitudes followed by a more gradual decline, giving it a sawtooth-like shape, whereas the other waveform does not contain these shock-like shapes. A subjective listening study has shown that a skewness of the time-derivative of a pressure waveform, or derivative skewness greater than three, $dSk > 3$, is indicative of the presence of crackle.[18,26] Using this model to predict crackle content, with dSk values of 14.4 and 0.3 for the shock-containing and non-shock-containing waveforms, respectively, the shock-containing waveform can be considered to contain crackle while the other does not.
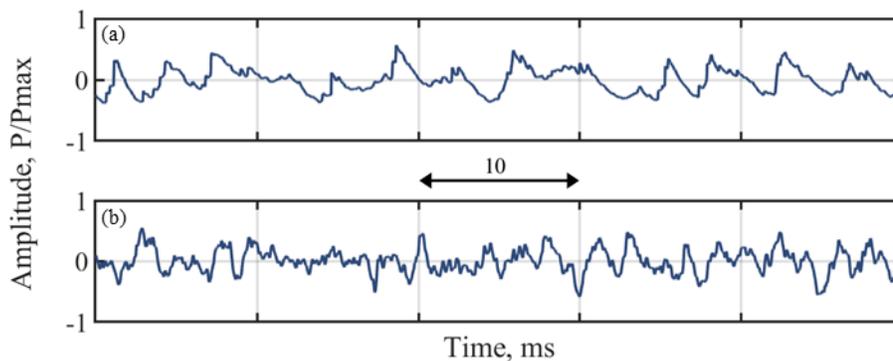

Figure 5. Waveform segments from the F-35B at 75% ETR, each 50-ms in length, that show (a) a shock-containing, crackling and (b) a non-shock-containing, non-crackling waveform. Amplitude is normalized by the maximum pressure value in each waveform.

In Fig. 6, two representations of the compiled normalized histograms across each of the microphone pairs for the apparent origin and propagation angle from the top 1000 events are shown for 75% ETR. A comparison between the events of interest are shown in Figs. 6a and 6c with

probabilities greater than 0.1 represented. For all the event types, the apparent source region and propagation inlet angles overlap, with the derivative events (yellow) being more compact than the top pressure events (green) and the largest pressure events being more compact than the evenly-space events (blue). This likely indicates that within a high-pressure event, a large derivative exists within the windowed waveform and vice versa. The evenly-spaced events having a broader, but similar apparent source region and propagation angle suggests that the occurrences of large derivatives and high-pressures occur often throughout the waveform. Therefore, with similar trends as the other event types, but with a more compact apparent origin and propagation angle, the results for the largest derivatives will be used for the remainder of the analysis to examine the apparent source location of crackle in the near field.

For both the apparent source location and propagation angle, a distinct separation occurs at approximately 3 m downstream. Upstream of this separation, propagation angles are less than 90°, meaning they propagate upstream from the jet axis to the microphone array, and downstream of this separation, angles are greater than 90° and propagate downstream. The apparent source region of microphones upstream of this separation is 3-5 m downstream along the jet axis and is partially associated with broadband shock-associated noise (BBSAN) which is a dominant source of noise in the forward direction.[27] Microphones downstream of the separation region have a more compact source region up to 10 m downstream along the microphone array with increasing propagation angles, shown in Figs. 6b and 6d. Beyond this, the source region broadens, however, changes in the propagation angle are minimal, potentially indicating a more consistent radiation angle towards the end of the array.
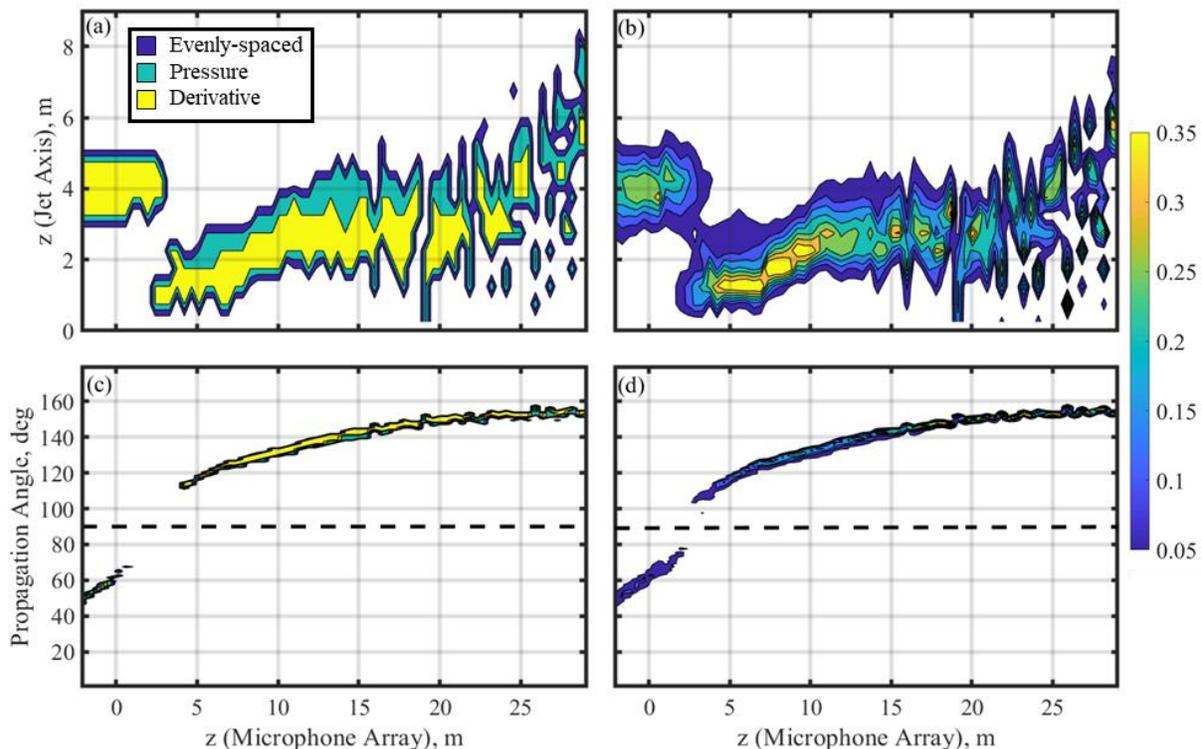
Figure 6. Comparisons of the (a) apparent origin and (c) propagation angle for the three-event types with densities greater than 0.1 and the normalized histograms of the (b) apparent origin and (d) propagation angle for the largest 1000 derivative events. The legend in (a) indicates the event types and applies to the event comparisons in (a) and (c), whereas the color bar on the right shows probability densities for the right two figures. In all figures, the x-axis is the z position along the microphone array, with the y-axis in (a) and (b) being the z position along the jet axis for the apparent origin. Dashed lines in (c) and (d) indicate 90°, about which propagation will be upstream at lower angles and downstream at greater angles.

Taking the top occurring propagation angle of the top 1000 derivative events for each adjacent microphone pair and tracing back to the jet centerline results in Fig. 7. This beamforming representation shows that the microphones experiencing forward radiating noise, likely from the BBSAN and fine-scale turbulent structures,[27] can easily be distinguished from the others. When traced to the jet centerline, the apparent source region of the top derivative events found along the microphone array exist entirely upstream of the MARP. There also appear to be groupings of other traced rays; however, they require further analysis to elucidate.
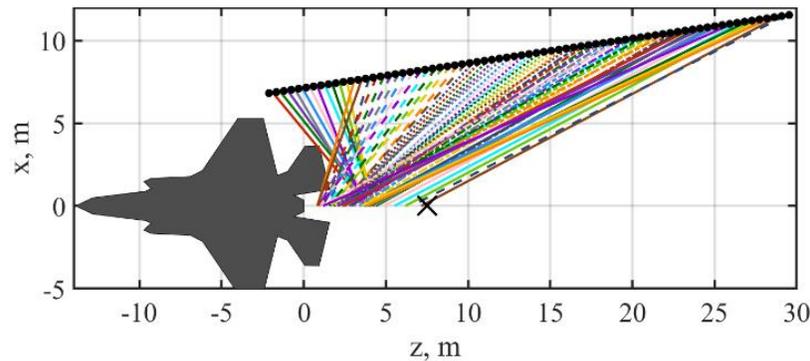

Figure 7. Geometry schematic with rays traced from the top occurring beamforming angle for each microphone pair to the apparent origin along the jet axis for 75% ETR.

Distinct groupings of propagating rays can be defined by taking the traced origins of the top 1000 derivative events and comparing to propagation angle, derivative skewness (dSk), and overall sound pressure level (OASPL) trends. The dSk and OASPL trends along the microphone array were averaged across six run-ups and are displayed in Figs. 8a and 8b. Variation in dSk is minimal at upstream locations while there is great variance at downstream locations, whereas there is less than ± 1 dB difference in OASPL across the run-ups. Colored shapes are used to represent each defined region in Fig. 8a and 8b with corresponding colored lines in Fig. 9. These colored regions are defined in Table 1 by propagation angle, dSk value, and OASPL. Angles less than 90° propagate upstream and angles less than 90° propagate downstream from the jet axis to the microphone array. Only the blue grouping has upstream propagation. Using the dSk model to predict crackle content,[18] waveforms with a dSk greater than 3 are considered to contain crackle, which applies to the green and yellow groupings. One significance of the OASPL criteria is to differentiate between the two peaks in the OASPL, indicated by the distinction of the green and yellow groupings. This multipeak occurrence in the OASPL coincides with the multilobe phenomenon seen in the F-35 noise field with the green and yellow region each being mainly attributed to a separate lobe.[28-30] However, the sudden increase in dSk observed at farthest aft angles is unexpected as spatial maps of dSk by James *et al.*[25] showed dSk values varying smoothly spatially for each engine condition as well as decreasing in the farthest aft direction. However, those results were for microphones located off the ground. One possible reason for increased derivative skewness values on the ground (corresponding to greater shock content) is irregular reflection and Mach stem formation, due to the high source amplitude and low angle of incidence. Fievet *et al.*[31] have shown the coalescence of shock waves in the near field, meaning there could be nonlinear interactions between waveforms. However, this hypothesis needs further investigation. Nonetheless, these four groupings now defined by propagation angle, dSk, and OASPL trends lend more insight into the spatial origins of the large-amplitude derivatives present at the array.

Table 1. Criteria for color groupings.

| Criteria	Blue	Red	Green	Yellow
Angle	$< 90°$	$> 90°$	$> 90°$	$> 90°$
dSk	< 3	< 3	> 3	> 3
OASPL	-10 dB	-6 dB	1st Peak	2nd Peak
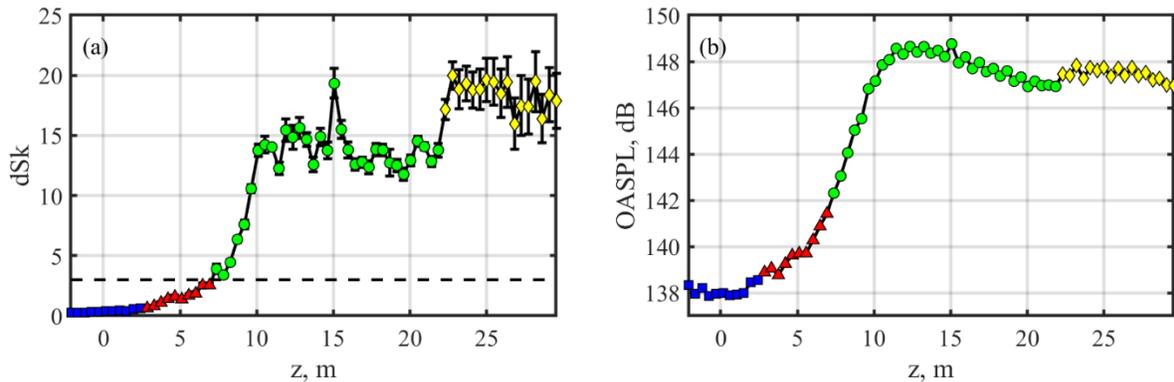
Figure 8. a) Derivative skewness (dSk) and b) overall sound pressure level (OASPL) values across the z-location along the microphone array. Four color groupings are shown, each with a distinct marker shape. Error bars for dSk indicate the standard deviation and a black dashed line is drawn at dSk = 3. OASPL levels have been normalized to a common distance of 20 m.

Apparent source regions of the top derivative events are now examined by grouping microphones based on dSk and OASPL trends shown in Figs. 8a and 8b to generate Fig. 9. The blue region relates to forward propagating noise that contains BBSAN and fine-scale turbulent structure noise,[27] but has very low dSk. Nevertheless, the highest derivative values in the (blue) forward-propagating region appear to originate from a compact region 3.6 – 4.5 m downstream of the nozzle, which corresponds to radiating angles shown in Fig. 6d of 46 – 76° relative to the jet inlet. With dSk < 3 and OASPL at least 6 dB below the peak, the red region also does not contain crackle according to the dSk model and appears to originate from a narrow region closest to the nozzle at a downstream distance of 0.8 – 1.6 m with 105 – 126° radiation angles. The green region has an apparent source region of 1.1 – 3.5 m, with its greatest concentration between 2.0 – 3.0 m, and with dSk > 3. This region corresponds to the maximum sound radiation direction with radiation angles of 126 – 150° and is a potential source location of crackle. Beyond 22 m on the microphone array lies the broader yellow region with even greater dSk and potential crackle content, which spans 1.2 – 7.2 m, with greater concentration from 3.5 – 7.2 m. This region also radiates most unidirectionally at angles between 150 – 157°, as seen by the flatter region at the end of the array in Fig. 8b. The downstream propagating yellow region overlaps with the upstream propagating blue region, while the green region does not intersect along the jet axis with the blue region, though the overlapping of regions may change when origins are traced to the jet lipline or the shear layer.

Table 2. Propagation angles and apparent source region along the jet axis for each of the color groupings.

	Blue	Red	Green	Yellow
Angle (deg)	$49 – 77°$	$105 – 126°$	$126 – 152°$	$150 – 156°$
Jet Axis (m)	3.6 – 4.5	0.8 – 1.6	1.1 – 3.5	1.2 – 7.2

With the jet diameter, D, on the order of 1 m, the distances in Fig. 9 approximate to downstream distances scaled by D. The distances can be compared with the apparent origin of large-amplitude acoustic impulses of a high-performance military aircraft observed by Schlinker *et al.*[7,8] using a directional microphone method. Those results indicated the peak of the probability densities for the origin of large-amplitude acoustic impulses along the jet axis to be 3 – 7 D downstream of the nozzle. Similarly, all apparent source regions of the top 1000 derivative events for each angle for 75% ETR originate upstream of the MARP, with the regions traced from the peak OASPL and dSk regions along the microphone array being most concentrated between 2.0 – 7.2 m.
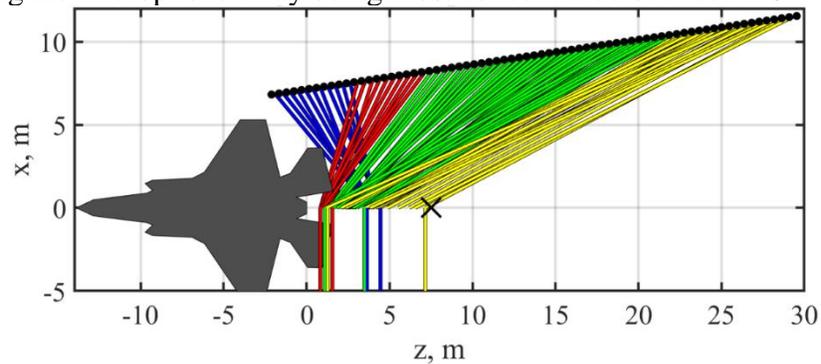
Figure 9. Modification of Fig. 7 according to the four regions identified in Fig. 8. Vertical colored lines at bottom indicate ranges of apparent origin locations for each color group.

5. CONCLUSION

This paper has examined the apparent source location of the top derivative events associated with the presence of crackle from a military aircraft for a single engine condition via an event-based beamforming method. Using a model developed from a subjective listening study correlating the presence of crackle with dSk, waveforms with a dSk greater than 3 were considered to contain crackle.[18] High derivative events correspond to high derivative skewness values which in turn relate to the presence of crackle. Comparing the source region of differing event triggers, the large derivative events have a more compact source region than largest pressure or evenly-spaced event. Apparent source regions of the top derivative events cluster together according to upstream or downstream propagation and trends in dSk and OASPL. The apparent origins are all found upstream of the MARP located at 7.5 m. The apparent crackle source region along the jet axis corresponding to the first peak in the OASPL (green) lies upstream of the apparent source region of the upstream propagating events (blue). However, the second peak region in the OASPL (yellow), which also propagates downstream, contains even higher dSk values and overlaps at the jet axis with the upstream propagating source region (blue) with as well as having a more consistent radiation angle with a broader source region. The apparent origin of the top 1000 derivative events appear to be consistent with the apparent acoustic source strength results along the jet axis found by Schlinker *et al.*[7,8] Future work will include analysis of the other crackle containing engine conditions, as well as further examination of the event-based beamforming method.

ACKNOWLEDGMENTS

REFERENCES

[1] J. E. Ffowcs Williams, J. Simson, and V. J. Virchis, " 'Crackle': An annoying component of jet noise," J. Fluid Mech. **71**, 2, 251–271 (1975). DOI:10.1017/S0022112075002558

[2] A. Krothapalli, L. Venkatakrishnan, and L. Lourenco, "Crackle: A dominant component of supersonic jet mixing noise," AIAA Paper 2000-2024 (2000). DOI:10.2514/6.2000-2024

[3] D. A. Buchta, A. T. Anderson, and J. B. Freund, "Near-field shocks radiated by high-speed free-shear flow turbulence," AIAA Paper 2014-3201 (2014). DOI:10.2514/6.2014-3201

[4] J. W. Nichols, S. K. Lele, F. E. Ham, S. Martens, and J. T. Spyropoulos, "Crackle noise in heated supersonic jets," *Journal of Engineering for Gas Turbines and Power*, **135**, 5, 051202 (2013). DOI:10.1115/1.4007867

[5] J. W. Nichols, S. K. Lele, and J. T. Spyropoulos, "The source of crackle noise in heated supersonic jets," AIAA Paper 2013-2197 (2013). DOI:10.2514/6.2013-2197

[6] R. Fievet, C. E. Tinney, and W. J. Baars, "Acoustic waveforms produced by a laboratory scale supersonic jet," AIAA Paper 2014-2906 (2014). DOI:10.2514/6.2014-2906

[7] R. H. Schlinker, S. A. Liljenberg, D. R. Polak, K. A. Post, C. T. Chipman, and A. M. Stern, "Supersonic jet noise source characteristics & propagation: Engine and model scale," AIAA Paper 2007-3623 (2007). DOI:10.2514/6.2007-3623

[8] J. Laufer, R. Schlinker, and R. E. Kaplan, "Experiments on supersonic jet noise," AIAA J. **14**, (1976). DOI:10.2514/3.61388

[9] P. Pineau and C. Bogey, "Study of the generation of shocks by high-speed jets using conditional averaging," AIAA Paper 2018-3305, June 2018. DOI:10.2514/6.2018-3305

[10] K. L. Gee, V. W. Sparrow, A. A. Atchley, and T. B. Gabrielson, "On the perception of crackle in high amplitude jet noise," *AIAA Journal,* Vol. 45, No. 3, 2007, pp. 593–598. DOI:10.2514/1.26484

[11] S. H. Swift and K. L. Gee, "Examining the use of a time-varying loudness algorithm for quantifying characteristics of nonlinearly propagated noise (L)," *Journal of the Acoustical Society of America*, Vol. 129, No. 5, 2011, pp. 2753–2756. DOI:10.1121/1.3569710

[12] S. H. Swift, K. L. Gee, and T. B. Neilsen, "Testing two crackle criteria using modified jet noise waveforms," *Journal of the Acoustical Society of America*, Vol. 141, No. 6, 2017, pp. EL549–EL554. DOI:10.1121/1.4984819

[13] K. L. Gee, T. B. Neilsen, and A. A. Atchley, "Skewness and shock formation in laboratory-scale supersonic jet data," *Journal of the Acoustical Society of America,* Vol. 133, No. 6, 2013, pp. EL491–EL497. DOI:10.11311/1.4807307

[14] S. Martens, J. T. Spyropoulos, and Z. Nagel, "The effect of chevrons on crackle—Engine and scale model results," in ASME Turbo Expo 2011 (2011). DOI:10.1115/GT2011-46417

[15] P. Mora, N. Heeb, J. Kastner, E. J. Gutmark, and K. Kailasanath, "Effect of heat on the pressure skewness and kurtosis in supersonic jets," *AIAA Journal*, Vol. 52, No. 4, 2014, pp 777–787. DOI:10.2514/1.J052612

[16] W. J. Baars and C. E. Tinney, "Shock structures in the acoustic field of a Mach 3 jet with crackle," *Journal of Sound and Vibration*, Vol. 333, No. 12, 2014, pp. 2539–2553. DOI:10.1016/j.jsv.2014.01.008

[17] K. L. Gee, T. B. Neilsen, A. T. Wall, J. M. Downing, M. M. James, R. L. and McKinley, "Propagation of crackle-containing noise from military jet aircraft," *Noise Control Engineering Journal* Vol. 64, No. 1, 2016, pp. 1–12. DOI:10.3397/1/376354

[18] P. B. Russavage, T. B. Neilsen, K. L. Gee, and S. H. Swift, "Rating the perception of jet noise crackle," Proc. Mtgs. Acoust. 33, 040001 (2018). DOI:10.1121/2.0000821

[19] K. L. Gee, P. B. Russavage, T. B. Neilsen, S. H. Swift, and A. B. Vaughn, "Subjective rating of the jet noise crackle percept," *Journal of the Acoustical Society of America*, Vol. 144, No. 1, 2018, EL40–EL44. DOI:10.1121/1.5046094

[20] K. L. Gee, T. B. Gabrielson, A. A. Atchley, and V. W. Sparrow, "Preliminary analysis of nonlinearity in military jet aircraft noise propagation," *AIAA Journal*, Vol. 43, No. 6, 2005 pp. 1398–1401. DOI:10.2514/1.10155

[21] K. L. Gee, V. W. Sparrow, M. M. James, J. M. Downing, C. M. Hobs, T. B. Gabrielson, and A. A. Atchley, "The role of nonlinear effects in the propagation of noise from high power aircraft," *Journal of the Acoustical Society of America*, Vol. 123, No. 6, 2008, pp. 4082–4093. DOI:10.1121/1.2903871

[22] K. L. Gee, J. M. Downing, M. M. James, R. C. McKinley, R. L. McKinley, T. B. Neilsen, and A. T. Wall, "Nonlinear evolution of noise from a military aircraft during ground run-up," AIAA Paper 2012-2258, June 2012. DOI:10:2514/6.2012-2258

[23] K. L. Gee, T. B. Neilsen, M. B. Muhlestein, A. T. Wall, J. M. Downing, M. M. James, and R. L. McKinley, "On the evolution of crackle in jet noise from high-performance engines," AIAA Paper 2013-2190, June 2013. DOI:10:2514/6.2013-2190

[24] W. J. Baars, C. E. Tinney, M. S. Wochner, and M. F. Hamilton, "On cumulative nonlinear acoustic waveform distortions from high-speed jets," *Journal of Fluid Mechanics*, Vol. 749, 2014, pp. 331–366. DOI:10.1017/jfm.2014.228

[25] M. M. James, A. R. Salton, J. M. Downing, K. L. Gee, T. B. Neilsen, B. O. Reichman, R. L. McKinley, A. T. Wall, and H. L. Gallagher "Acoustic Emissions from F-35B Aircraft during Ground Run-Up," AIAA Paper 2015-2375, June 2015. DOI:10.2514/6.2015-2375

[26] B. O. Reichman, M. B. Muhlestein, K. L. Gee, T. B. Neilsen, and D. C. Thomas, "Evolution of the derivative skewness for nonlinearly propagating waves," *Journal of the Acoustical Society of America*, Vol. 139, No. 3, 2016, pp. 1390–1403. doi:10.1121/1.4944036

[27] T. B. Neilsen, A. B. Vaughn, K. L. Gee, S. H. Swift, A. T. Wall, J. M. Downing, and M. M. James, "Inclusion of broadband shock-associated noise in spectral decomposition of noise from high-performance military aircraft," *AIAA/CEAS Aeroacoustics Conference, 2018.* DOI:10.2514/6.2018-3146

[28] K. M. Leete, A. T. Wall, K. L. Gee, T. B. Neilsen, M. M. James, and J. M Downing, "Dependence of high-performance military aircraft noise on frequency and engine power," AIAA Paper 2018-2826, June 2018. DOI:10.2514/6.2018-2826

[29] S. H. Swift, K. L. Gee, T. B. Neilsen, A. T. Wall, J. M. Downing, and M. M. James, "Spatiotemporal correlation analysis of jet noise from round-nozzle supersonic aircraft," AIAA Paper 2018-3938, June 2018. DOI:10.2514/6.2018-3938

[30] S. H. Swift, K. L. Gee, T. B. Neilsen, A. T. Wall, J. M. Downing, and M. M. James, "Spatiotemporal analysis of high-performance military aircraft noise during ground run-up," *Journal of the Acoustical Society of America,* Vol. 142, No. 4, 2017, pp. 2512-2512, 2017. DOI:10.1121/1.5014174

[31] R. Fievet, C. E. Tinney, W. J. Baars, and M. F. Hamilton, "Coalescence in the sound field of a laboratory-scale supersonic jet," AIAA Journal, Vol. 54, No. 1, 2016, pp. 254-265. DOI: 10.2514/1.J054252